Hydrobiologia manuscript No.
(will be inserted by the editor)

The large scale impact of offshore wind farm structures on pelagic primary productivity in the southern North Sea

Kaela Slavik · Carsten Lemmen · Wenyan Zhang · Onur Kerimoglu · Knut Klingbeil · Kai W. Wirtz

Received: date / Accepted: date

This research is funded by the Marine, Coastal and Polar Systems (PACES II) of the Hermann von Helmholtz-Gemeinschaft Deutscher Forschungszentren e.V.. K.S. is funded by the European Commission Erasmus Mundus Masters Course in Environmental Sciences, Policy and Management (MESPOM). C.L., O.K. and K.K. received support from the "Modular System for Shelves and Coasts" (MOSSCO) grant provided by the Bundesministerium für Bildung und Forschung under agreements 03F0667A and 03F0667B; O.K. and K.W. are also supported by the DFG priority programme 1704 "Flexibility matters: Interplay between trait diversity and ecological dynamics using aquatic communities as model system" (DynaTrait) under grant agreement KE 1970/1-1. K.K. is furthermore supported by the DFG Collaborative Research Center "Energy Transfers in Atmosphere and Ocean" TRR181. We thank all co-developers of the model coupling framework MOSSCO, foremost M. Hassan Nasermoaddeli and Richard Hofmeister. The authors gratefully acknowledge the computing time granted by the John von Neumann Institute for Computing (NIC) and provided on the supercomputer JURECA at Forschungszentrum Jülich. We are grateful to the open source community that provided many of the tools used in this study, including but not limited to the communities developing ESMF, FABM, GETM and GOTM.

K. Slavik
Helmholtz Zentrum Geesthacht Zentrum für Material- und Küstenforschung, Germany
Present address: Future Earth Paris Global Hub, Université Pierre et Marie Curie, France

C. Lemmen
Helmholtz Zentrum Geesthacht Zentrum für Material- und Küstenforschung, Germany
Corresponding author
Tel.: +49 4152 87-2013
Fax: +49 4152 87-2020
E-mail: carsten.lemmen@hzg.de

W. Zhang, O. Kerimoglu, K.W. Wirtz
Helmholtz Zentrum Geesthacht Zentrum für Material- und Küstenforschung, Germany

K. Klingbeil
Universität Hamburg, Germany and Leibniz-Institut für Ostseeforschung Warnemünde, Germany

Abstract The increasing demand for renewable energy is projected to result in a 40-fold increase in offshore wind electricity in the European Union by 2030. Despite a great number of local impact studies for selected marine populations, the regional ecosystem impacts of offshore wind farm structures are not yet well assessed nor understood. Our study investigates whether the accumulation of epifauna, dominated by the filter feeder *Mytilus edulis* (blue mussel), on turbine structures affects pelagic primary productivity and ecosystem functioning in the southern North Sea. We estimate the anthropogenically increased potential distribution based on the current projections of turbine locations and reported patterns of *M. edulis* settlement. This distribution is integrated through the Modular Coupling System for Shelves and Coasts to state-of-the-art hydrodynamic and ecosystem models. Our simulations reveal non-negligible potential changes in regional annual primary productivity of up to 8% within the offshore wind farm area, and induced maximal increases of the same magnitude in daily productivity also far from the wind farms. Our setup and modular coupling are effective tools for system scale studies of other environmental changes arising from large-scale offshore wind-farming such as ocean physics and distributions of pelagic top predators.

Keywords Offshore wind farm · primary productivity · North Sea · MOSSCO · modular coupling · biofouling

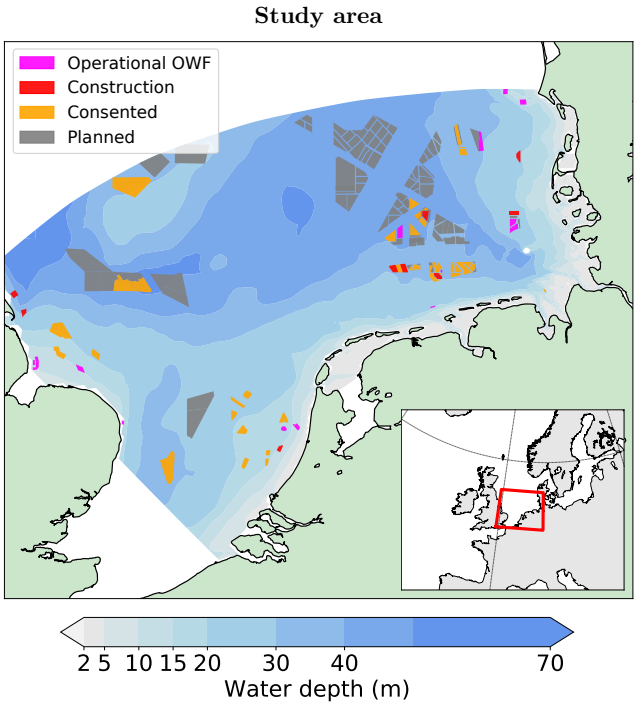

Fig. 1 Study (and model) domain in the Southern North Sea with distribution of offshore wind farms (OWFs, data from Ho et al 2016). Color indicates the planning status of each OWF as of September 2015 where parks in operation and under construction are shown in magenta and red color, and foreseen constructions with consented or planned status in orange and gray color. For our scenario analysis, we consider a maximum exploitation that assumes that all shown OWFs are in operation by 2030.

1 Introduction

Recognition of the role of burning fossil fuels in anthropogenic climate change has led to increased investment in renewable energy such as wind farming (Edenhofer et al 2011). In particular, offshore wind energy has proliferated over the past decade and will be integral in the transition to renewable energy systems. In the European Union (EU), offshore wind farms (OWFs) are predicted to increase 13-fold between 2015 and 2020, and 40-fold by 2030, in order to meet 4.2% of EU total electricity consumption (Global Wind Energy Council 2015).

Currently, 63% of OWFs in EU waters are concentrated in the southern North Sea (SNS), with the remainder located in the Atlantic Ocean and Baltic Sea. The SNS is expected to remain a hotspot for EU OWF development, where ≈ 85% of OWFs are currently under construction and ≈ 75% of OWFs have received consent (Ho et al 2016). Offshore wind turbines are solid structures, typically larger than their onshore counterparts, built of steel or concrete, with monopiles accounting for 80%. OWFs are being built further offshore and in deeper waters, with the average water depth increasing three-fold and the average distance from shore five-fold between 1991 and 2010 (Kaldellis & Kapsali 2013). The large additional build-up of OWFs by 2030 is evident from the spatial distribution of operational, under construction, consented and planned OWFs in the SNS (Fig. 1).

The increasing number of OWFs alters the functioning of the surrounding pelagic ecosystem by restructuring the biological communities at and around the submerged foundations and pile structures (Joschko et al 2008; Krone et al 2013). Specifically, they increase the biomass and distribution of filter feeders (Krone 2012; Lindeboom et al 2011), because OWFs provide the hard substrate needed for colonisation by a variety of epistructural species. This colonisation is also referred to as biofouling. Among the colonisers, the bivalve *Mytilus edulis* (L. 1758, Bivalvia: Mytilidae) is the dominant species near the water surface (Table 1) (Freire & Gonzalez-Gurriaran 1995; Riis & Dolmer 2003; Wilhelmsson & Malm 2008; Joschko et al 2008; Krone et al 2013). For example, piles of the OWF research platform FINO 1 (Forschungsplattformen in Nord- und Ostsee) are covered by an average of 4300 kg of *M. edulis*, with a turnover rate of more than 50% of the stock per year (Krone et al 2013).

Biofouling not only generates habitat for a new epistructural community, i.e. biota that live on and attach to a structure, but it has further consequences for the benthic community underneath and the surrounding pelagic zone (Krone 2012; Maar et al 2009). Filter feeders have been shown to significantly reduce the ambient concentration of phytoplankton and of micro- and mesozooplankton (Dolmer 2000; Maar et al 2007), which to some extent likely applies to epistructural *M. edulis* as well (Maar et al 2009). By changing phytoplankton biomass, epistructural filtration can be expected to affect primary productivity and thus the very basis of the marine food web and biogeochemical cycling locally above mussel beds and around the offshore wind turbine.

Our study aims to assess the sensitivity of pelagic primary productivity to changed abundance and distribution of *M. edulis* on OWFs for an entire regional-scale ecosystem. It is the first study to investigate the accumulated effects on primary productivity at the systems scale, beyond the local impacts of individual offshore wind turbines. Prerequisites for such an assessment are (i) the reconstruction of*M. edulis* abundance both for their natural, epibenthic habitat and for the new epistructural niches; (ii) the functional coupling of the lateral and vertical distribution of reconstructed mussels to phytoplankton prey fields in a realistic hy-

Table 1 Offshore wind farms in the Southern North Sea where *M. edulis* are the dominant species.

Country	Location	Reference
Germany	FINO 1 research platform	Krone et al 2013
Belgium	C-Power OWF	Kerckhof et al 2012
Netherlands	Egmond aan Zee OWF	Bouma & Lengkeek 2012; Lindeboom et al 2011
Denmark	Horns Rev OWF	Leonhard et al 2006
Sweden	West coast of Sweden	Langhamer et al 2009

drodynamic and biogeochemical representation of the SNS.

For the integrated modelling of benthic and epistructural filtration, water physics and pelagic biogeochemistry, we use the recently introduced modular framework by Lemmen et al (2018), which contains a novel ecosystem model recently applied to and verified for the SNS by Kerimoglu et al (2017). Multi-annual simulations run with and without epistructural mussels allow a first estimate of the sensitivity of pelagic primary productivity to the projected OWFs in this regional sea.

2 Materials and Methods

2.1 Study location

The southern North Sea (SNS) is located between 51° N and 56° N and is bordered by the United Kingdom, Belgium, the Netherlands, Germany and Denmark (Fig. 1). The water is fairly shallow with an average depth of 30 m and comprises an extended area of intertidal flats and several major estuaries (Eisma & Kalf 1987). The seabed is composed predominantly of sand and, in the deeper and more coastal parts, of mud (Walday & Kroglund 2002). The SNS experiences strong seasonal variability, with winter storms often generating large surface waves and suspending greater amounts of sediments (Groll & Weisse 2017; Nasermoaddeli et al 2017). Currents in the North Sea are generated by tides and wind forcing, with the latter especially important during storm events (Howarth 2001). The North Sea obeys a general cyclonic circulation. This is driven by prevailing westerly winds, residual tidal currents and the baroclinic pressure gradient set up by coastal river discharge (e.g., Otto et al 1990). The residual circulation within the basin flows southward along the east coast of the UK, before turning west in the East Anglia plume and then continuing westward along the West Frisian barrier islands. Part of the residual current then continues northward towards Norway. The other part continues along the East Frisian barrier islands and joins the Elbe and Weser River inflows. It then turns northwest again towards the central North Sea, bypassing Helgoland Island, before turning back towards and flowing north along the Danish coastline (Carpenter et al 2016).

2.2 Reconstruction of spatial distribution of epibenthic *M. edulis*

Open access spatial data on the abundance and distribution of *M. edulis* were obtained from the Joint Nature Conservation Committee (JNCC), the Ocean Biogeographic Information System (OBIS), the Archive for Marine Species and Habitats Data (DASSH), the Global Biodiversity Information Facility (GBIF) and the Belgian Marine Data Centre (BMDB). Most of the data (43%, rounded) was from JNCC, 26% and 23% from BMDC and GBIF (containing presence only data), and 9% from OBIS. Only few data points came from DASSH $< 1\%$. Removing duplicate locations, in total 4074 count observations and 37 214 presence only data were used for the reconstruction of the spatial distribution of epibenthic *M. edulis*.

To extrapolate and interpolate the count and occurrence data to the entire domain of the SNS, we used empirical relationships between mussel abundance, sediment grain size and depth. We added to this a low abundance random distribution for deep water and a constant high abundance for mussel beds. As *M. edulis* are tolerant to large variations in temperature (0–29 °C) and salinity (Seed & Suchanek 1992), such factors were not considered in the reconstruction. Taking the average adult *M. edulis* individual biomass as 600 mg dry weight (DW) (Bayne & Worrall 1980), which equals 64.5 mg ash-free dry weight (AFDW, Ricciardi & Bourget 1998, Table 2), the abundance and distribution of *M. edulis* in the SNS was spatially reconstructed using the median sediment grain size map that is publicly available from the NOAH habitat atlas (www.noah-project.de/habitatatlas/).

M. edulis prefers larger sediment grain sizes and hard substrate (OSPAR Commission 2010), thus an increase in abundance density (n) with increasing sediment grain size, ranging from an abundance of $1\,\mathrm{m}^{-2}$ in muddy areas (median grain size $d_{50} < 0.06$ mm) to $40\,\mathrm{m}^{-2}$ in areas of coarse gravel, at locations where mussels are found. We employed a Random Forest model

(Liaw & Wiener 2002) to create a predictor of abundance density from median grain size. Comparison to Wadden Sea field data compiled by Compton et al (2013), however, indicated that predicted shallow-water mussel abundance was greatly overestimated, which can be attributed to a positive sampling bias in the citizen-science data set. We thus interpreted the count data as relative, i.e. as a probability of occurrence that needs to be rescaled to conform to the Compton et al (2013) estimate where it borders the Wadden Sea, and rescaled the data accordingly.

The abundance–sediment grain size relationship is applied up to a 10 m natural depth limitation (Reise & Schubert 1987; Suchanek 1978). Outside the depth limitation, *M. edulis* still occur, however at a much reduced density, and are often completely absent: A random density between $0\,m^{-2}$ and $0.5\,m^{-2}$ is assigned. In the Wadden Sea, no sediment data is available in the NOAH data set, and a constant value of $2\,m^{-2}$ is assigned on the Wadden flats consistent with Compton et al (2013). Mussel beds were incorporated as point data using the OSPAR Biodiversity Committee habitat classification, where a constant density of $3911\,m^{-2}$ (Nielsen & Maar 2007) is downscaled to $170\,m^{-2}$ to account for the patchiness of the beds.

Presence only data is not a preferred estimator for species distribution modelling, especially when there is a sampling bias. Many of the GBIF-reported *M. edulis* observations are opportunistic finds reported by citizen scientist divers, with a bias towards more accessible near-coast areas and towards summer temperature. This bias may be overcome by environmental constraints that can serve as proximate absence (Phillips et al 2009), such as water depth for *M. edulis*. We note that the epibenthic reconstruction of abundance presented here is preliminary. As it serves as a baseline only, the uncertainty in this epibenthic reconstruction does not harm the results obtained for the ecosystem sensitivity (see Sect. 2.3). We are currently working on a refined epibenthic reconstruction that address the effect of this uncertainty on the baseline itself (Lemmen, North Sea ecosystem-scale quantification of primary productivity changes by the benthic filter feeder *Mytilus edulis*, unpublished manuscript).

2.3 Epistructural *M. edulis*

The biomass and species diversity of epistructrual communities at OWFs are much higher than would be found on natural hard substrate (Wilson & Elliott 2009), with species composition varying with both depth and time, as recorded at both FINO 1 (Krone et al 2013; Joschko et al 2008), and the Kentish Flats OWF (Bessel 2008).

Table 2 *M. edulis* biomass with depth, averaged over all years 2005–2007 sampled by Krone et al (2013, , pp. 4–5).

Depth (m)	Distribution (%)	range biomass density (kg m^{-2})	mean biomass total (kg)
0.0 – 2.5	95	22.3–43	3258.08
2.5 – 7.5	3	0.5–3.9	58.58
7.5 – 15	2	n/a	19.29
15.0 – 30.0	n/a	0	1.63

M. edulis is the dominant macrofauna species at shallower depths, while at greater depths Anthozoa and *Jassa spp.* are more prolific; other major taxa such as green algae, *Asterias rubens* (Asteroidea), Bryozoa, Porifera and *Tubularia spp.* are also present (Krone et al 2013). *M. edulis* is the most abundant and ecologically important species at OWF epistructrual communities in the North Sea (Table 1 and Borthagaray & Carranza 2007), contributing up to 90% of epistructural biomass in some locations. It is therefore also the main driver of ecological change around offshore structures (Krone et al 2013; Maar et al 2009).

The additional settlement of *M. edulis* as a result of OWFs is considered by incorporating the vertical distribution observed by Krone et al (2013) at the FINO 1 OWF. *M. edulis* abundance (n) at an offshore wind turbine is a function of its radius (r) and its base depth (z), with the radius assumed to be 3 m at all OWFs (Orbis Energy Centre 2013). The influence of *M. edulis* on water properties is assumed to be equal around the entire circumference, without consideration of current direction. Multiplying the abundance density by the circumference gives the vertical distribution of *M. edulis* with depth at offshore wind turbines (Table 2). The abundance density over depth at each offshore wind turbine was calculated by converting the wet weight reported by Krone et al (2013) to DW using a factor of 6.6% and assuming $600\,mg\,DW\,ind^{-1}$ (Ricciardi & Bourget 1998; Bayne & Worrall 1980). We did not consider annual variation despite observed seasonal variations in the data set by Krone et al (2013) because mussel biomass sampled at different seasons over the years 2005–2007 were not found to be significantly different.

2.4 Spatial subgrid distribution

The spatial distribution of current and projected OWFs in the southern North Sea (Fig. 1) was overlaid on a curvilinear grid later used for the numerical model. Epibenthic areal abundance of *M. edulis* was considered to be (vertically) equally distributed within the lower-

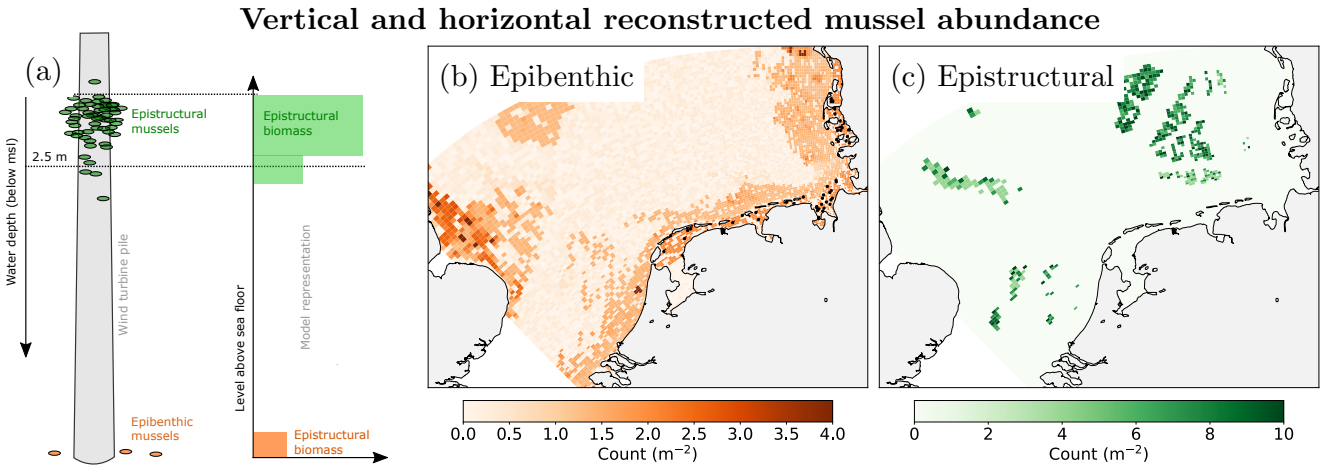

Fig. 2 (a) Vertical representation of epibenthic and epistructural *M. edulis* as observed (left) and in the model space (right). Epibenthic mussels are homogeneously distributed in the lowermost model layer. Epistructural mussels are equally distributed in all model layers above 2.5 m depth, and proportionally in the model level encompassing the 2.5 m depth contour. No mussels are considered in the intermediate layers. (b) Reconstructed abundance of *M. edulis* at the sea floor, estimated from presence and count data and sediment habitat mapping; mussel beds with uniform abundance 170 m^{-2} shown as black dots. (c) Abundance on wind turbine piles, estimated from scaling individual pile monitoring observations to the coarse model grid.

most representable physical layer in the grid of the hydrodynamic model. Epistructural areal abundance was vertically distributed in all simulation layers representing the upper 2.5 m of the water column in the hydrodynamic model (Fig. 2a).

Estimating abundance density at OWFs from the abundance at individual turbines requires consideration of the turbine density at OWFs. Offshore wind turbines are often spaced between five and eight times the rotor diameter (E.ON Climate & Renewables 2011), which tend to range from 80 to 100 m (International Renewable Energy Agency 2012). Assuming a rotor diameter of 100 m and a spacing of five times this distance, this means that each offshore wind turbine requires 500 m spacing or 0.25 km^2 area, giving an average wind turbine density of 4 km^{-2}.

2.5 Coupled model system

Extrapolation from the compiled OWF locations to the entire SNS area and the description of *M. edulis* influence on the pelagic ecosystem requires a spatially explicit, coupled model approach, for which we employ the recently developed open source software infrastructure Modular System for Shelves and Coasts (MOSSCO, www.mossco.de, Lemmen et al 2018). MOSSCO facilitates the exchangeable coupling of models and data sets and enables the integration of modules describing physical, chemical, geological, ecological and biogeochemical processes. MOSSCO applications for the 3D coastal ocean focus on processes at the benthic–pelagic interface and, among others, explain spatio-temporal patterns in coastal nutrient concentration (Hofmeister et al 2017; Kerimoglu et al 2017), primary productivity (Kerimoglu et al 2017), macrobenthic biomass and community dynamics (Zhang & Wirtz 2017) and suspended sediment concentration as affected by macrobenthic activities (Nasermoaddeli et al 2017).

MOSSCO features generic output and input components that can be used to integrate, e.g., river nutrient fluxes, open ocean boundary conditions and faunal abundance. As a physical driver within MOSSCO, we employed the coastal ocean model GETM (General Estuarine Transport Model, Burchard et al 2002; Klingbeil & Burchard 2013) to calculate sea level, currents, temperature and salinity distributions, and to transport the biogeochemical and ecological quantities. GETM obtains state-of-the-art turbulence closure from the General Ocean Turbulence Model (GOTM, Umlauf & Burchard 2005), and has been shown to have high skill in various studies for the North Sea and SNS (e.g. Gräwe et al 2016; Purkiani et al 2016).

Pelagic ecology was described by the Model for Adaptive Ecosystems in Coastal Seas (MAECS, Wirtz & Kerimoglu 2016) implemented as a FABM module; MAECS simulates pelagic nutrient, phytoplankton, zooplankton and detritus dynamics and accounts for the acclimation of intracellular composition in phytoplankton. In our application, MAECS resolves the elements carbon (C), nitrogen (N), and phosphorus (P), and features

adaptive shifts in phytoplankton ecophysiology as described by, e.g., variable chlorophyll a (Chl-a) and RuBisCO contents. The underlying scheme for these adaptive shifts has been derived as an optimality theory and was first applied to phytoplankton growth and succession by Wirtz & Eckhardt (1996). Pelagic element fluxes are described similar to other ecosystem models including nutrient uptake during phytoplankton growth, transformation through phytoplankton mortality including herbivorous grazing, and stoichiometrically controlled turnover of detritus and dissolved organic matter in terms of C, N, and P.

A full description and an extensive performance assessment of the model for a decadal hindcast of the SNS has been provided by Kerimoglu et al (2017). Our coupled setup differs in two respects: (i) we resolve filtration (see Sect. 2.5.1), and (ii) we used the full 3D biogeochemical model OmexDia based on Soetaert et al (1996) instead of the the single layer soil parameterization by Kerimoglu et al (2017). There, top-down mortality of zooplankton is uniform, while we prescribe higher zooplankton mortality near the coast. Furthermore, the ecosystem model MAECS has since evolved and now includes a parameterization for viral loss of phytoplankton (Wirtz 2018, Physics or biology? Persistent chlorophyll accumulations in a shallow coastal sea explained by pathogens and carnivorous grazing, submitted manuscript, hereinafter referred to as Wirtz, submitted).

2.5.1 Filtration model

M. edulis actively passes water over a specialized filtering structure (the gill), thereby removing a significant proportion of both organic (i.e., mainly phytoplankton) and inorganic particles with high efficiency (Widdows et al 1979). The volume of water passed over the gill area per unit of time and individual body volume is referred to as the clearance rate (CR). CR has been observed to increase with rising current velocity (Cranford & Hill 1999). At very low ambient Chl-a concentration below about $0.5\,\mathrm{mg\,m^{-3}}$, however, CR ceases for energetic reasons (Riisgård et al 2003). The removal of particles from the cleared water, termed the filtration rate (FR), depends, among others, on the concentration and organic quality of particles. A physiological regulation of filtration rate is, however, debated and has been studied for high ambient food concentrations only. At the concentrations typically found in the SNS, full exploitation of the ambient concentration can be expected (Clausen & Riisgård 1996; Asmus & Asmus 1991).

Our model implementation of *M. edulis* FR is based on the empirical relations identified by Bayne et al (1993). They formulated the relationship in terms of phytoplankton carbon amount concentration ($[C]$) and total particulate matter (TPM) relative to an assumed individual DW of 300 mg.

$$\mathrm{FR}_{\mathrm{TPM},300} = 0.05 \cdot [C]^{0.983}, \quad (1)$$

The following assumptions for the conversion of coefficients and carbon units were used: we (i) take the experimentally-determined organic matter fraction of 56% (average over all experiments in Bayne et al 1993 of measured particulate organic matter (POM) to TPM); (ii) use carbon mass to molar ratio with of 12.011 mg $\mathrm{mmol^{-1}}$; (iii) use dry weight (DW), ash free dry weight (AFDW) and wet weight conversions from Ricciardi & Bourget (1998); (iv) apply molar mass conversion in Redfield stoichiometry (molar ratio 106:16:1 C:N:P) to express the DW to amount carbon ratio as 32.43 mg per mmol C; (v) scale all rates to individual mass 600 mg with the experimentally confirmed metabolic scaling exponent of 0.67 (Bayne & Worrall 1980; Bayne et al 1993). As a lower threshold for filtration, a phytoplankton carbon concentration of $[\mathrm{C}]_{\mathrm{min}} = 0.7\,\mathrm{mmol\,m^{-3}}$ was chosen, consistent with the threshold suggested by Riisgård et al (2003) of 0.5 mg Chl-a $\mathrm{m^{-3}}$. Filtration of phytoplankton biomass by *M. edulis* removes particulate carbon, nitrogen, and phosphorus from the pelagic phytoplankton compartment, in the same stoichiometric proportion as the food, and with it also reduces dependent phytoplankton properties like Chl-a. The phytoplankton compartment is converted to detritus, representing faeces and pseudofaeces, in carbon, nitrogen and phosphorous. We assume that 20% of the carbon is lost to respiration, leading to higher quality ejected detritus compared to the food source; direct DIN (e.g., urea, see Cockcroft e.g., 1990) release by mussels is not considered.

The filtration model is technically realised as an Earth System Modeling Framework (ESMF, Hill et al 2004) component and coupled with MOSSCO (Lemmen et al 2018) to the Framework for Aquatic Biogeochemical Models (FABM, Bruggeman & Bolding 2014) with the MAECS biogeochemical model in the pelagic and OmexDia (Soetaert et al 1996) with added phosphorous cycle (Hofmeister et al 2014) in the soil FABM domains.

2.5.2 Model setup and scenarios

The SNS was represented on a curvilinear grid with cell size between 2 and 64 $\mathrm{km^2}$, with the highest resolution in the German Bight. Vertically, the water column was represented by 20 terrain-following σ-layers (Kerimoglu et al 2017). The model setup accounts for the discharge of freshwater, phosphorous and nitrogen from major

Table 3 Scenarios contrasted in this study

Scenario	Description	Total biomass
REF	Presence of epibenthic mussels. This represents the reference state against which the addition of artificial hard substrate by OWFs is compared.	$16 \cdot 10^{11}$ indiv. 96 tons
OWF	As REF, but with additional presence of epistructural mussels in pelagic surface layers.	$7 \cdot 10^{10}$ indiv. 42 tons

rivers into the southern North Sea, including the Elbe, Weser, Ems, Rhine, Meuse, Scheldt and Humber (see Kerimoglu et al 2017). Tidal sea surface elevation was forced at the open ocean boundary. Open ocean boundary conditions for nutrients in dissolved and particulate forms were obtained from a North Atlantic shelf simulation with ECOHAM (Ecosystem Model Hamburg, Große et al 2016) and provided as a 10 year climatology Kerimoglu et al (2017). Phytoplankton and zooplankton were assumed to be at zero-gradient at the boundaries. The meteorological forcing was obtained from the long-term Climate Limited area Model reconstruction available in the CoastDat database (Geyer 2014).

Simulations were run for the duration for 14 consecutive years 2000-2013, with the first three years discarded to allow for a model spin-up, especially for the equilibration of winter nutrient storage in the sediment. As we are evaluating a sensitivity for a projected year 2030 scenario, the choice of this period is arbitrary and reflects availability of station and satellite data for model evaluation. Two different scenarios were compared, (1) presence of only epibenthic mussels (scenario "REF"), and (2) additional presence of epistructural *M. edulis* at OWFs, focussed within the upper pelagic layers (scenario "OWF") (Table 3).

The filtration model was configured with phytoplankton carbon as the main species to filter, with co-filtration of phytoplankton nitrogen, phosphorous, Chl-a and rubisco. The model diagnostic rates of relative carbon uptake were multiplied by phytoplankton carbon concentration and subsequently integrated for the entire year to obtain the annual net primary productivity. The 3D time step of the hydrodynamic model was 6 minutes. Data exchange between the different components of the model system was performed every 30 minutes. The bottom roughness length was constant at $z_0 = 0.002\,\mathrm{m}$, wave forcing was disabled. A Jerlov Type III water class was used for the radiation scheme.

2.6 Data for model evaluation

No observational data is available for primary productivity at the scale of the SNS. Rather than productivity as a rate, the stock of phytoplankton is readily observed with *in situ* methods or by remote sensing. We evaluate Chl-a as simulated by the model against station observations of chlorophyll fluorescence along three transects and against synoptic satellite observations of ocean color.

Time series of near-surface Chl-a concentration were obtained from the Dutch authority Rijkswaterstaat through the OpenEarth portal (Rijkswaterstaat 2017). From all available station data, we selected three transects that cross the coastal nutrient gradient from nearshore Noordwijk, Terschelling and Rottumerplat to up to 235 km offshore. Satellite observations were obtained from the European Space Agency Ocean Color Climate Change Initiative (ESA-CCI version 3.1), a multi-platform combined product of Chl-a concentration.

3 Results

The reconstructed abundance of *M. edulis* in the SNS suggests $1.6 \cdot 10^{11}$ individuals on natural (benthic) substrate and within mussel beds (Fig. 2b) The reconstructed accumulated biomass of benthic *M. edulis* in the SNS amounts to total mussel mass of 96 Mt DW (or 10 Mt AFDW). For the potential "artificial" stock at offshore wind turbines, the reconstructed abundance (Fig. 2c) in the entire SNS amounts to $7.0 \cdot 10^{10}$ individuals, or 42 Mt DW (4.5 Mt AFDW). Once all the planned wind farms are in operation, they will provide habitat for mussels that are equal to 44% of the stock of benthic mussels.

3.1 Uncertainty estimates of reconstruction

The reconstruction of mussel abundance in the southern North Sea is based on analysis of field data (in total 4074 count observations and 37 214 presence only data, which reveals a positive correlation ($r = 0.78$) between abundance and sediment grain size. The 10 m water depth line is introduced to provide a pseudo-absence criterion. To test a sensitivity of the reconstruction result to the water depth limitation, we also calculated the abundance using 25 m water depth contour line (≈95% of observed presence occurs within this water depth) as an alternative constraint, which leads to an increase in abundance by $\approx 1.4 \cdot 10^{10}$ compared to that using the 10 m. This amounts to ≈9% of the total budget estimated using the 10 m water depth constraint,

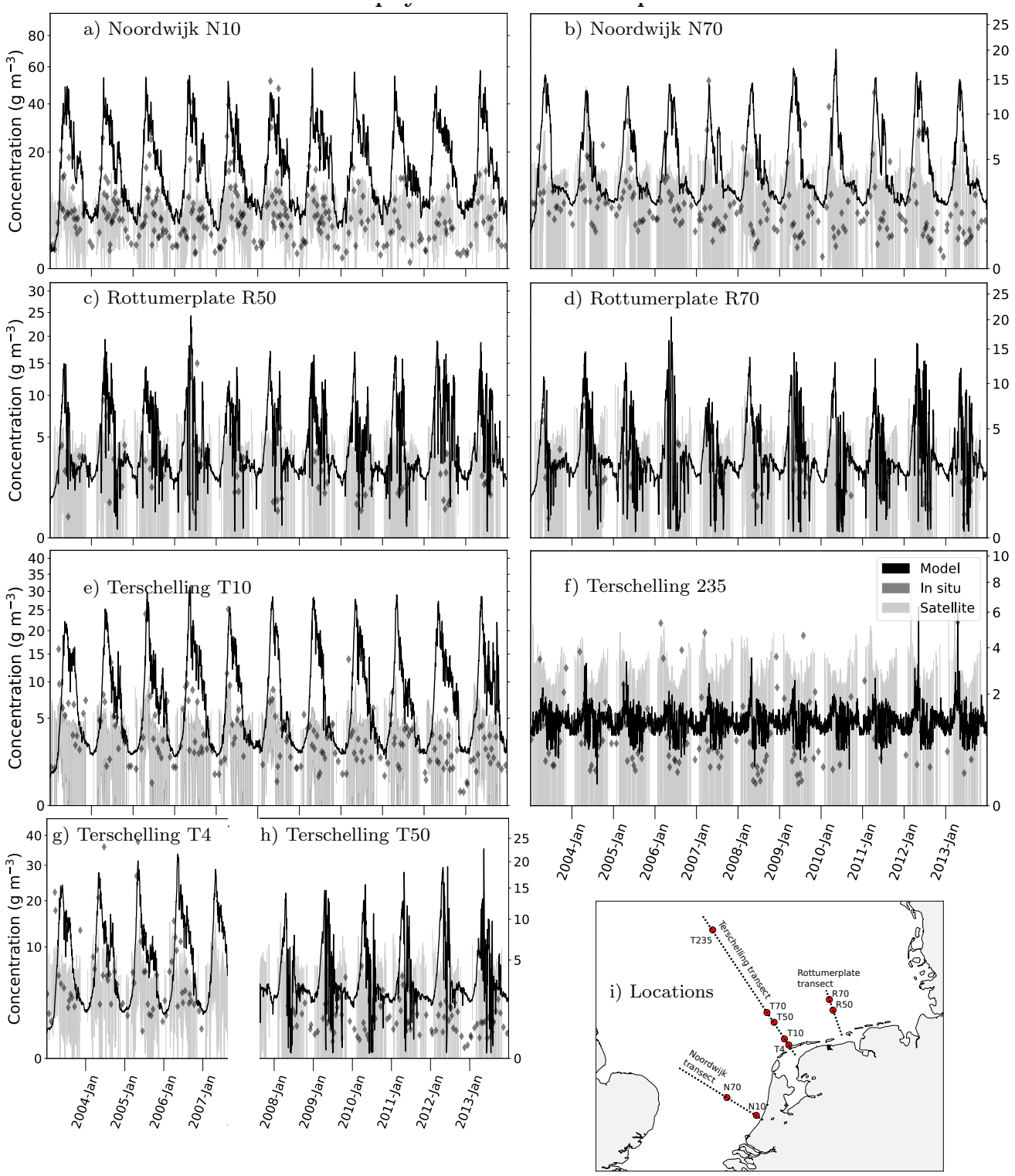

Fig. 3 Comparison between in situ measurements (diamonds), satellite observations (gray line) and simulations (black line) of surface chlorophyll for three coastal transects "Noordwijk" (a,b), "Terschelling" (e–h) and "Rottumerplate" (c,d), where numbers denote distance from coast (e.g., R10 = 10 km off Rottumerplate). Stations T4 and T50 did not provide in-situ data for part of the time series. The satellite gridded observation and the simulation from scenario REF were sampled in a 5000 m radius around the respective station location (i). Data from Rijkswaterstaat and European Space Agency (CCI v3.1 product).

and thus does not affect our estimation to a large degree. The area covered by mussel beds in the Wadden Sea oscillated annually between $6.2 \cdot 10^7$ and $3 \cdot 10^7\,m^2$ since 1998 (Nehls et al 2009). Since our estimation of the stock in the Wadden Sea is based on a maximum value, the annual oscillation of mussel beds would affect the total estimated budget in the SNS by 10% at most: our reconstruction and the annual fluctuation should be within 30% of the total estimated budget, taking into account oscillations of the mussel beds and the impact of extreme wind waves on offshore wind turbines, which might occasionally clear all mussels from a wind turbine (Krone et al 2013).

3.2 Simulated chlorophyll and comparison to station/statellite data

Simulated surface Chl-a for the years 2003–2013 exhibits a typical annual phytoplankton cycle with a large spring bloom and a smaller summer bloom. At the bloom peak, the Chl-a concentration reaches 20–50 mg m^{-3} at coastal and below $5\,mg\,m^{-3}$ at far offshore locations (Fig. 3). The simulation reproduces *in situ* time series of near-surface Chl-a concentration along the three transects from Noordwijk, Terschelling and Rottumerplate. The peak spring bloom Chl-a concentrations are well matched across the entire coastal gradient; overall the simulation has a small positive bias below 4 mg m^{-3}, with a larger overestimation of 9 mg m^{-3} at Noordwijk 10. The variability of Chl-a concentrations is also well represented. At most stations, the simulated and the observed standard deviation agree to within 1.2 mg m^{-3}, with the exception of Terschelling 10 and Noordwijk 10, where the model standard deviation is 3 mg m^{-3} higher than the observed variability.

The comparison against satellite observations shows that both model and *in situ* observations have a wider temporal variability, while the mean Chl-a concentration is again well represented. The model surface Chl-a climatology, i.e. the multi-annual average over all years 2003–2013, has a small positive bias compared to satellite observations: it is below or near 1.0 mg m^{-3} in fall and winter, and largest during May, when simulated Chl-a is 3.6 mg m^{-3} larger on average. This difference is smallest (below 1 mg m^{-3}) offshore and where most of the OWF are located. It is largest (up to 15 mg m^{-3}) in the near-shore high-productivity zone along the East and West Frisian barrier islands.

3.3 Net primary productivity

The simulated annual vertically integrated net primary productivity (NPP, expressed as carbon productivity) in the SNS, as well as the climatological average over the years 2003–2013, broadly separates the model domain into three regions (Fig. 4): (1) the coastal area including the Wadden Sea, of highly variable and low vertically integrated carbon production ($< 50\,g\,m^{-2}\,a^{-1}$, very shallow and turbid water), (2) the near-coast transition zone with a high productivity above $180\,g\,m^{-2}\,a^{-1}$ up to $\approx 400\,g\,m^{-2}\,a^{-1}$, and (3) the offshore SNS, again with relatively low productivity around $90\,g\,m^{-2}\,a^{-1}$.

This pattern is consistent across all simulation years. Maximum productivity in this simulation occurs in an elongated coast-following area 20 km north and east of the West Frisian and East Frisian islands, in the central Southern Bight, and off the East coast of England. Within the period 2003–2013, the year 2010 exhibits the lowest productivity with $118 \pm 47\,g\,m^{-2}\,a^{-1}$, and the it is highest in 2003 ($142 \pm 52\,g\,m^{-2}\,a^{-1}$). Most OWF are located in the transition zone between the maximum productivity band and the low productivity areas offshore.

There is less primary productivity locally in the OWF than in the REF scenario in all years (Fig. 5). The maximum loss occurs within the OWF areas (up to 8%), and is on average $3.7 \pm 1.5\%$, with a maximum in 2005 and 2010 (4.1%) and a minimum in 2008 (3.3%). Variability is high between the different OWF areas with a climatological standard deviations of 1.5%). Loss outside the OWF areas is much smaller, but the change is consistently negative and $0.4 \pm 2.5\%$) in the long-term mean. This outside-OWF loss also has a typical distribution with largest losses in the maximum productivity band along the East and West Frisian barrier islands and in the vicinity of the OWF. In many years, productivity is increased (a very small increase below 1%) along the North Frisian barrier islands.

To identify a regional effect outside the OWFs, we identified the maximum increase and maximum decrease of daily NPP between the scenarios for each year (Fig. 3.3, shown for 2006). The maximum daily decrease of NPP is $-11 \pm 9\,mmol\,C\,m^{-3}\,d^{-1}$, with the largest decreases (below $-20\,mmol\,C\,m^{-3}\,d^{-1}$) occurring within the two large clusters of OWF areas in the eastern SNS. The spatial distribution of the maximum daily increase of NPP shows changes of the same order of magnitude throughout the SNS ($11 \pm 12\,mmol\,C\,m^{-3}\,d^{-1}$). In contrast, however, maximum increases also occur outside the OWF areas, with the largest increases (above $20\,mmol\,C\,m^{-3}\,d^{-1}$) east of the central eastern SNS OWF cluster and also bear the East Frisian and North Frisian barrier islands.

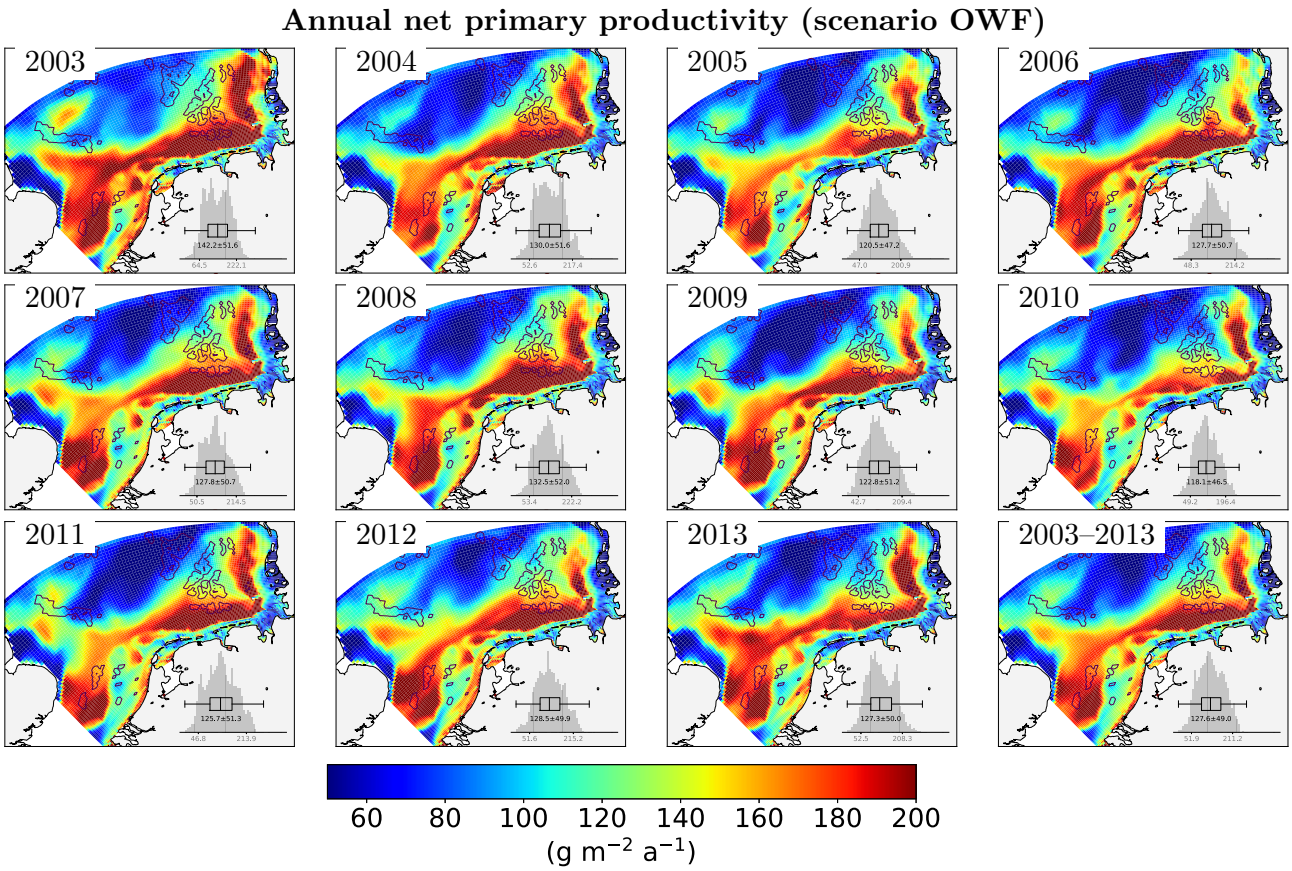

Fig. 4 Simulated annual net primary productivity 2003–2013. Contours denote areas with OWF epistructural *M. edulis*.

The maximum increase is seen up to 50 km away from the farms.

4 Discussion

Net primary productivity calculated by our coupled model shows low productivity in the Wadden Sea area (Fig. 4). Simulated Chl-a concentrations in this area are also lower than those estimated by the satellite imagery (e.g., Kerimoglu et al 2017; Ford et al 2017), while in the open SNS, our model modestly overestimates Chl-a and probably also NPP. NPP simulated by van Leeuwen et al (2013) with the same hydrodynamic (GETM) but with a different ecosystem model (ERSEM, Baretta et al 1995) is much higher (on average $318 \pm 29\,\mathrm{g\,m^{-2}\,a^{-1}}$) than NPP simulated here for their region termed "SNS", referring to a small area of the Southern Bight of the North Sea. While this is not a good choice of region for comparison, because the exact location of this maximum productivity region varies between the years (Fig. 4), also their entire North Sea estimate of $180 \pm 10\,\mathrm{g\,m^{-2}\,a^{-1}}$ is higher than our calculation. When comparing the two studies, however, one should note that they averaged over the much higher trophic state period 1985–2005, such that lower productivity should be expected for the period 2003–2013.

Already Emeis et al (2015) report values around $200\text{–}270\,\mathrm{g\,m^{-2}\,a^{-1}}$, for an area corresponding to our coastal high productivity region in the year 2002, based on the Ecosystem Model Hamburg (ECOHAM, Pätsch & Kühn 2008). The comparison by van Leeuwen et al (2013) with *in situ* observation derived NPP estimates by Weston (2005), however, also showed that their model under- or overestimates observations by a factor of two depending on the area type (stratified, frontal bank), and overestimated surface mixed layer productivity by up to a factor of five (van Leeuwen et al 2013, Table 1). Given these considerations the simulated productivity in the coastal and open SNS (ranging between 50 and $400\,\mathrm{g\,m^{-2}\,a^{-1}}$) is plausible. Its skill needs to be assessed against observational data in forthcoming studies, such as Wirtz (submitted) .

In contrast to productivity, biomass related variables are readily observable from a variety of platforms: the agreement between the *in situ* measured, the remote sensing observed, and the simulated Chl-a concentrations (Fig. 3) suggests that phytoplankton dynamics

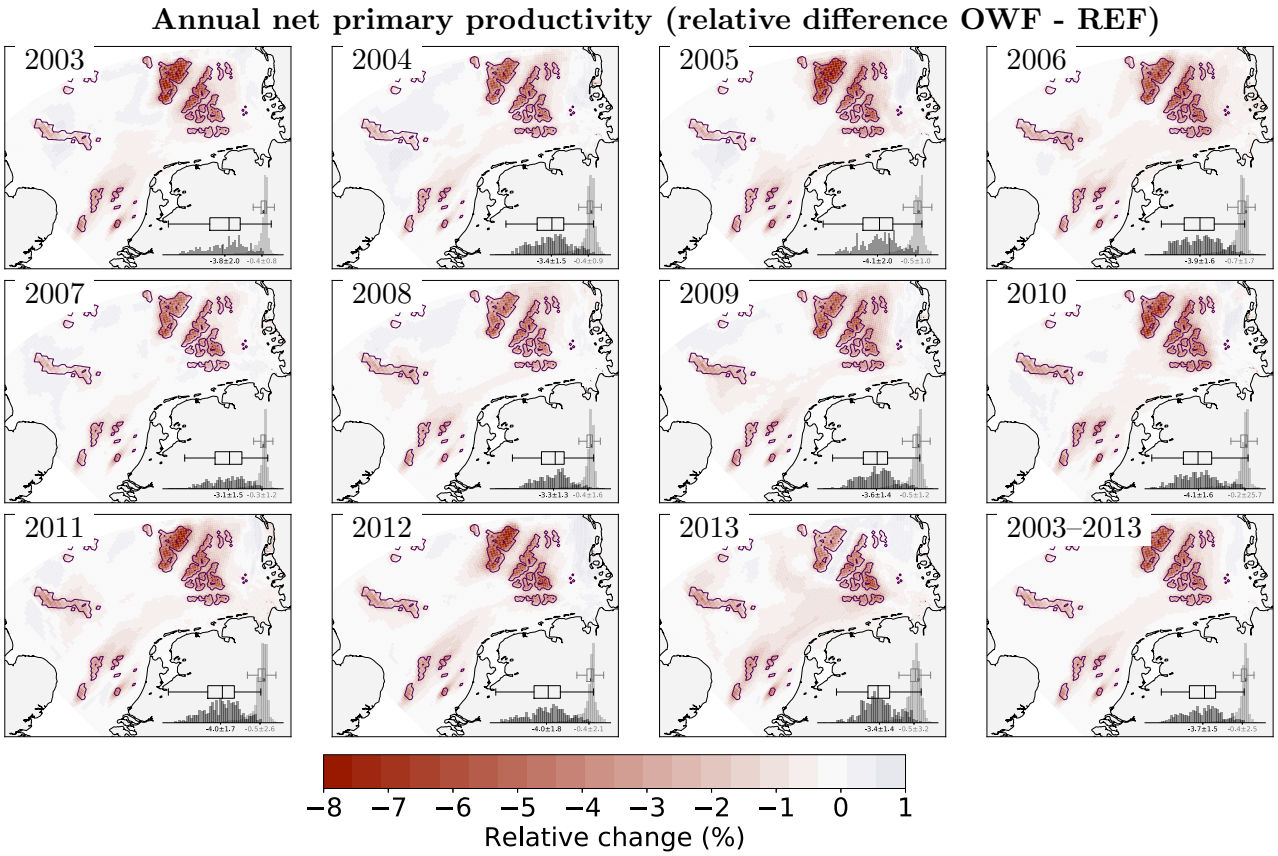

Fig. 5 Simulated relative difference of annual net primary productivity 2003–2013 and climatological between simulations with and without epistructural mussels, calculated as $100 \cdot (\mathrm{OWF} - \mathrm{REF})\,/\mathrm{REF}$.

is well reproduced, which builds confidence in the representation of primary productivity by the model. Moderate discrepancies in the cross-coastal distribution of NPP and Chl-a are in part due to the simplified description of water attenuation by high concentrations of suspended particles close to the coast (Kerimoglu et al 2017) and the prescribed mortality gradient of zooplankton. However, given that the concentrations are in the range where mussel filtration exhibits a linear functional response to food concentration, the moderate mismatch should not affect our estimates of the relative effects of additional epistructural filtration.

4.1 Non-local spatial effects

During a bloom, phytoplankton will usually first appear at the surface and then sink down through the water column (Cloern 1996), producing a delay between surface phytoplankton concentrations and those at depths. Similarly, the phytoplankton loss from epistructural filtration is first and clearly visible at the surface, where *M. edulis* are concentrated, before being transmitted into the entire water column. After filtration, nutrients that were bound in phytoplankton are readily made available by pelagic remineralization of the ejected high-quality detritus. By this mechanism, it is to be expected that filtration sustains a longer bloom through faster nutrient recycling and also supports higher productivity in regions that receive nutrient-enriched and phytoplankton reduced water masses from OWF areas by currents.

The maximum daily NPP changes (Fig. 3.3) indeed demonstrate that the ecosystem effect of epistructural filtration is not a local one, but a regional one, with a decrease of phytoplankton carbon throughout many parts of the SNS (albeit concentrated up to 20 km around the OWF) and a strong increase up to 50 km outside the OWF area. It can be argued that the magnitude of several percent per year in overall draw-down is well within the uncertainty range of state-of-the-art ecosystem models. The effect is, however, regionally very different and thus changes horizontal gradients in productivity that have not been discussed before: there is a notable impact of projected epistructural suspension feeders on the ecosystem functions of a regional

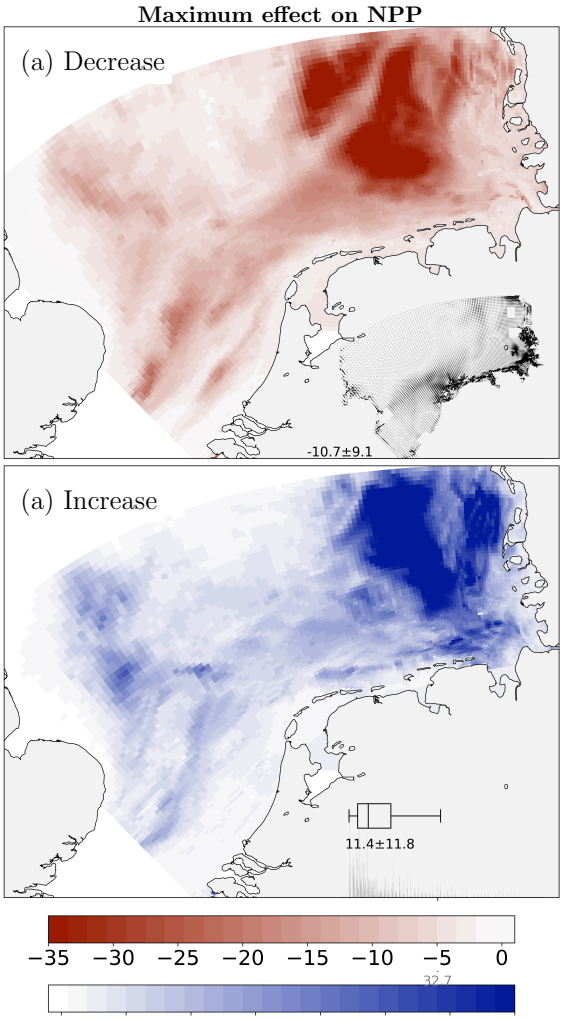

Fig. 6 Maximum daily net primary productivity effect of epistructural *M. edulis* (exemplary for year 2006). (a) Maximum decrease in 2006, and (b) maximum increase in 2006.

shelf sea. Even though the decrease in primary productivity is relatively small, it extends over a large area and intensifies in close proximity to OWFs, reaching a maximum reduction in annual net primary productivity of 8%. Despite the dilution of meso-scale mussel density due to the low area density of offshore wind turbines, massive biofouling accumulates to an effect size which is only one order of magnitude lower than the 60% reduction within shellfish aquacultures (Waite 1989).

4.2 Altered ecological functioning

Primary productivity represents the major energy source for ecosystems globally (Imhoff et al 2004). Our model results indicate that the construction of OWFs reduces available primary productivity, especially at the local scale, as a result of a higher abundance of filter feeders (Prins et al 1997). Filtration activity transforms the carbon, nutrient and energy flows at OWFs from which the benthic food-web benefits, with faeces, pseudofaeces and dead mussels enriching the benthic organic pool, as observed in many shellfish aquaculture facilities worldwide (e.g. Cranford et al 2007). Notably, filter feeding much accelerates the transformation of living biomass into partially dissolved and bio-available nutrients, which may again fuel productivity. The effects on autotrophic standing stock investigated in our study hence do not provide a full account of processes relevant for assessing primary productivity.

Our results suggest that the increased abundance of *M. edulis* at OWFs only moderately affects ecosystem functioning. They emphasize *M. edulis*'s role as an ecosystem engineer (Borthagaray & Carranza 2007), not just locally but on a scale of greater than 50 km. Pelagic primary productivity is just one of many facets of ecosystem functioning, which have been hypothesized to be altered by OWFs (amongst others):

1. Networks of OWFs are beneficial for the conservation of threatened species by acting as *de facto* marine protected areas (Inger et al 2009). Access to most areas designated as OWFs is limited, primarily for safety reasons, which limits anthropogenic pressures such as fishing, including bottom trawling, potentially leading to an increased level of biodiversity at OWFs as compared to unprotected areas (Kaiser et al 2006; Tillin et al 2006; Inger et al 2009).

2. Mussels such as *M. edulis* play a significant role in modifying the natural substrate and increasing species richness (Borthagaray & Carranza 2007). *M. edulis* bioengineers its surrounding environment through shell litter fall (White & Pickett 1985), water filtration and clarification (Newell 2004), concentration of nutrients (van Broekhoven et al 2014), ultimately increasing the species diversity and landscape heterogeneity as a result of structural and functional effects (Norling & Kautsky 2007). Shells, both dead or living, increase the degree of habitat complexity, encouraging a higher level of species richness (White & Pickett 1985). Bivalve and gastropod shells are persistent and abundant physical structures which provide substrata for attachment and refuge from predation as well as physical or physiological stress (Gutiérrez et al 2003).

3. Mediated through the associated epibenthic community, OWF constructions can act as stepping stones for the dispersal of exotic species (Glasby et al 2007). The artificial habitat is open for colonization by new species assemblages (Wilson & Elliott 2009), which could not quickly establish in soft-bottom sea regions. One

example of this is *Telmatogeton japonicus*, the marine splash midge, which is native to Australasian waters. Known to be transported on the hulls of ships, it has been observed at OWFs in Denmark and along the Swedish Baltic coast (Wilhelmsson & Malm 2008). The projected density of offshore constructions will likely facilitate immigration by non-native species (Bulleri & Airoldi 2005), such as the leathery sea squirt (*Styela clava*), slipper limpet (*Crepidula fornicate*), pacific oyster (*Crassostrea gigas*) and Japanese skeleton shrimp (*Caprella mutica*) (Buschbaum & Gutow 2005; Diederich et al 2005; Lützen 1999; Thieltges et al 2003). Through these changes in biodiversity, OWFs could shape the marine ecosystem beyond their physical boundaries.

4. *M. edulis* are a highly diverse prey source capable of supporting higher trophic levels, especially vagile demersal megafauna (e.g. fish like *Trisopterus luscus* and crabs like *Cancer pagurus*) (Langhamer et al 2009; Reubens et al 2011). Their abundance and distribution at OWFs is driven by changes in attraction, productivity and redistribution (Bohnsack 1989). An increase in the population of vagile demersal megafauna further impact the local community, leading to increased species diversity (Wilhelmsson & Malm 2008). Larger megafauna may also benefit from increased food availability (e.g., Brasseur et al 2012), with seals extending their distribution towards an OWF after construction in Denmark (Tougaard et al 2006).

Many of the ecosystem feedbacks and hence changes to ecosystem services are yet unknown and need to be studied both *in situ* and in future system-wide synoptic studies. Mostly for supporting the planning process, a high number of often not published studies were conducted, almost always considering individual offshore wind turbines and focused on selected potential effects such as on birds, megafauna, or hydrodynamics (Bailey et al 2014, e.g.).

4.3 Limitations and outlook

This study is the first large scale assessment of epistructural *M. edulis* filtration at OWFs. The level of quantification achieved in our study clearly shows that at least with respect to primary productivity there is a non-negligible regional ecosystem effect originating from epistructural *M. edulis* filtration. Modular model systems are needed to integrate effects and feed-backs across trophic levels and up to the regional scale, as proposed and to a large but not complete degree realised here.

There are still large uncertainties related to simulating complex ecosystem interactions. The reconstruction of filter feeder epistructural abundance is yet a simple up-scaling of data sampled from single piles. And the benthic reconstruction suffers from the sampling bias introduced by opportunistic observations. These data issues will likely ameliorate in the future with monitoring programs and systematic surveys. The filtration model is very simple and does not include, for example, age structured population dynamics or nutrient recycling: this study shows how essential it is to improve filtration models, which so far are often neglected in shelf ecosystem models. For studies adressing the forthcoming decades, a more accurate quantification of the epistructural filtration effect seems to be required. Physical effects of wind farm on atmospheric boundary layer circulation and ocean currents and vertical mixing (e.g. McCombs et al 2014; Carpenter et al 2016) have not been considered by our coupled model: there is still a scale problem that needs to be addressed in physical modelling to bridge the wind pile (order of 10 m) to ecosystem (order of 100 km) scales. Recent developments in nested or unstructured models seem promising here. Last but not least, the uncertainties of the simulation result are difficult to quantify: estimates of productivity in the literature have large uncertainties themselves. There are no regional studies to which the filtration rates can be compared. Our findings of a 8% annual productivity and up to 30mmol $\mathrm{C\,m^{-3}\,d^{-1}}$daily productivity justify further research into the large-scale impact of OWFs. Remote sensing observations might provide the first regional direct observations of OWF effects as the resolution of the sensors now allows the identification of single wind turbines, as has already been done for physical parameters (Platis et al 2018).

5 Conclusions

Construction of offshore wind farms (OWFs) in the southern North Sea is predicted to continue into the future, highlighting the importance of understanding the potential nature and magnitude of the environmental impact of the epistructural biomass known to accumulate on their subsurface structures. Epistructural communities at OWFs in the southern North Sea are dominated by *M. edulis*, a filter feeder capable of inducing extensive ecological change through filtration, amongst other processes. The construction of all currently planned, consented and under construction OWFs, in addition to those already in operation, is likely to increase the overall abundance of *M. edulis* in the southern North Sea by more than 40%. In addition to providing an additional food source and a new habitat, *M. edulis* also remove phytoplankton from the water column through filtration, which impacts ecosystem functioning.

Reconstructing and analysing the impact of epistructural biomass at OWFs on pelagic primary productivity at a larger spatial scale, in this case the southern North Sea, provides valuable insights into ecosystem functioning which are not visible at the scale of a single offshore wind turbine or OWF. The impact of OWFs on annual primary productivity is predominately local, at short time scales there is a larger regional effect on biomass and productivity that extends up to several 100s of km beyond the bounds of the OWF area.

Code and data availability

Development code and documentation are hosted on Sourceforge (https://sf.net/p/mossco/code) The release version 1.0.3 is permanently archived and accessible under the digital object identifier https://doi.org/10.5281/zenodo.1243045. All external software used is available as open source and can be obtained together with MOSSCO. The simulations were performed in parallel on 192 cores on the Jureca high performance computer at Forschungszentrum Jülich, Germany (Krause & Thörnig 2016).

Satellite data are freely available from the Ocean Colour Climate Change Initiative dataset, Version 3.1, European Space Agency, at http://www.esa-oceancolour-cci.org/. Meteorological forcing data are available on request from CoastDat at www.coastdat.de (Geyer 2014). Chlorophyll a and other water quality parameters are freely available at http://www.waterbase.nl (Rijkswaterstaat 2017).

The reconstructed epibenthic and epistructural *M. edulis* maps (Fig. 2) and the simulated net primary productivity data for both scenarios (Figs. 4, 5) have been archived with PANGAEA — Data Publisher for Earth & Environmental Science as the dataset "Simulated net primary productivity (NPP) in the southern North Sea 2003-2013 forced by epistructural and epibenthic reconstructed blue mussel filtration". They are available under the digital object identifier https://doi.org/XXXXXX.XXXX.

References

Asmus RM, Asmus H (1991) Mussel beds: limiting or promoting phytoplankton? Journal of Experimental Marine Biology and Ecology 148(2):215–232, DOI 10.1016/0022-0981(91)90083-9

Bailey H, Brookes KL, Thompson PM (2014) Assessing environmental impacts of offshore wind farms: lessons learned and recommendations for the future. Aquatic Biosystems 10(1):8, DOI 10.1186/2046-9063-10-8

Baretta JW, Ebenhöh W, Ruardij P (1995) The European Regional Seas Ecosystem Model (ERSEM), a complex marine ecosystem model. Netherlands Journal of Sea Research 33(3/4):233–246

Bayne BL, Worrall CM (1980) Growth and Production of Mussels Mytilus edulis from Two Populations. Marine Ecology Progress Series 3:317–328, DOI 10.3354/meps003317

Bayne BL, Iglesias J, Hawkins AJS (1993) Feeding behaviour of the mussel, Mytilus edulis: responses to variations in quantity and organic content of the seston. Journal of the Marine Biological Association of the United Kingdom 73(4):813–829

Bessel A (2008) Kentish Flats Offshore Wind Farm Turbine Foundation Faunal Colonisation Diving Survey. Report No. 08/J/1/03/1034/0839. Tech. rep., Kentish Flats Limited, Southampton

Bohnsack JA (1989) Are high densities of fishes at artificial reefs the result of habitat limitation or behavioral preference? Bulletin of Marine Science 44(2):631–645

Borthagaray AI, Carranza A (2007) Mussels as ecosystem engineers: Their contribution to species richness in a rocky littoral community. Acta Oecologica 31(3):243–250, DOI 10.1016/j.actao.2006.10.008

Bouma S, Lengkeek W (2012) Benthic communities on hard substrates of the offshore wind farm Egmond aan Zee (OWEZ). Tech. rep., Noordzeewind, Ijmuiden

Brasseur S, Aarts G, Meesters E (2012) Habitat preferences of harbour seals in the Dutch coastal area: Analyses and estimate of effects of offshore wind farms. Tech. rep., Institute for Marine Resources and Ecosystem Studies, Wageningen

van Broekhoven W, Troost K, Jansen H (2014) Nutrient regeneration by mussel Mytilus edulis spat assemblages in a macrotidal system. Journal of Sea Research 88:36–46

Bruggeman J, Bolding K (2014) A general framework for aquatic biogeochemical models. Environmental Modelling and Software 61:249–265, DOI 10.1016/j.envsoft.2014.04.002

Bulleri F, Airoldi L (2005) Artificial marine structures facilitate the spread of a non-indigenous green alga, Codium fragile ssp. tomentosoides, in the north Adriatic Sea. Journal of Applied Ecology 42(6):1063–1072, DOI 10.1111/j.1365-2664.2005.01096.x

Burchard H, Bolding K, Rippeth TP, Stips A, Simpson JH (2002) Microstructure of turbulence in the northern North Sea : a comparative study of observations and model simulations. Journal of Sea Research 47:223 – 238

Buschbaum C, Gutow L (2005) Mass occurrence of an introduced crustacean (Caprella cf. mutica) in the southeastern North Sea. Helgoland Marine Research 59:252–253, DOI 10.1007/s10152-005-0225-7

Carpenter JR, Merckelbach L, Callies U, Clark S, Gaslikova L, Baschek B (2016) Potential Impacts of Offshore Wind Farms on North Sea Stratification. PLOS ONE 11(8):e0160,830, DOI 10.1371/journal.pone.0160830

Clausen I, Riisgård HU (1996) Growth, filtration and respiration in the mussel Mytilus edulis: No evidence for physiological regulation of the filter-pump to nutritional needs. Marine Ecology Progress Series 141(1-3):37–45, DOI Doi10.3354/Meps141037

Cloern JE (1996) Phytoplankton bloom dynamics in coastal ecosystems: A review with some general lessons from sustained investigation of San Francisco Bay, California. Reviews of Geophysics 34(2):127–168, DOI 10.1029/96RG00986

Cockcroft A (1990) Nitrogen excretion by the surf zone bivalves Donax serra and D. sordidus. Marine Ecology

Progress Series 60:57–65, DOI 10.3354/meps060057
Compton TJ, Holthuijsen S, Koolhaas A, Dekinga A, ten Horn J, Smith J, Galama Y, Brugge M, van der Wal D, van der Meer J, van der Veer HW, Piersma T (2013) Distinctly variable mudscapes: Distribution gradients of intertidal macrofauna across the Dutch Wadden Sea. Journal of Sea Research 82:103–116, DOI 10.1016/j.seares.2013.02.002
Cranford P, Hill P (1999) Seasonal variation in food utilization by the suspension-feeding bivalve molluscs Mytilus edulis and Placopecten magellanicus. Marine Ecology Progress Series 190:223–239, DOI 10.3354/meps190223
Cranford P, Strain P, Dowd M, Hargrave B, Grant J, Archambault Mc (2007) Influence of mussel aquaculture on nitrogen dynamics in a nutrient enriched coastal embayment. Marine Ecology Progress Series 347:61–78, DOI 10.3354/meps06997
Diederich S, Nehls G, van Beusekom JE, Reise K (2005) Introduced Pacific oysters (Crassostrea gigas) in the northern Wadden Sea: Invasion accelerated by warm summers? Helgoland Marine Research 59(2):97–106, DOI 10.1007/s10152-004-0195-1
Dolmer P (2000) Feeding activity of mussels Mytilus edulis related to near-bed currents and phytoplankton biomass. Journal of Sea Research 44(3-4):221–231, DOI 10.1016/S1385-1101(00)00052-6
Edenhofer O, Pichs Madruga R, Sokona Y, Seyboth K (2011) Renewable energy sources and climate change mitigation. Tech. rep., Intergovernmental Panel on Climate Change, Cambridge
Eisma D, Kalf J (1987) Distribution, organic content and particle size of suspended matter in the North Sea. Netherlands Journal of Sea Research 21(4):265–285, DOI 10.1016/0077-7579(87)90002-0
Emeis KC, van Beusekom J, Callies U, Ebinghaus R, Kannen A, Kraus G, Kröncke I, Lenhart HJ, Lorkowski I, Matthias V, Möllmann C, Pätsch J, Scharfe M, Thomas H, Weisse R, Zorita E (2015) The North Sea A shelf sea in the Anthropocene. Journal of Marine Systems 141:18–33, DOI 10.1016/j.jmarsys.2014.03.012
EON Climate & Renewables (2011) E.ON Offshore Wind Energy Factbook. Tech. rep., E.ON Climate & Renewables, Essen
Ford DA, van der Molen J, Hyder K, Bacon J, Barciela R, Creach V, McEwan R, Ruardij P, Forster R (2017) Observing and modelling phytoplankton community structure in the North Sea. Biogeosciences 14(6):1419–1444, DOI 10.5194/bg-14-1419-2017
Freire J, Gonzalez-Gurriaran E (1995) Feeding ecology of the velvet swimming crab Necora puber in mussel raft areas of the Ría de Arousa (Galicia, NW Spain). Marine Ecology Progress Series 119:139–154
Geyer B (2014) High-resolution atmospheric reconstruction for Europe 19482012: coastDat2. Earth System Science Data 6(1):147–164, DOI 10.5194/essd-6-147-2014
Glasby TM, Connell SD, Holloway MG, Hewitt CL (2007) Nonindigenous biota on artificial structures: could habitat creation facilitate biological invasions? Marine Biology 151(3):887–895, DOI 10.1007/s00227-006-0552-5
Global Wind Energy Council (2015) Global Wind Report 2015: Annual Market Update. Tech. rep., Global Wind Energy Council, Brussels
Gräwe U, Flöser G, Gerkema T, Duran-Matute M, Badewien TH, Schulz E, Burchard H (2016) A numerical model for the entire Wadden Sea: Skill assessment and analysis of hydrodynamics. Journal of Geophysical Research: Oceans 121(7):5231–5251, DOI 10.1002/2016JC011655
Groll N, Weisse R (2017) A multi-decadal wind-wave hindcast for the North Sea 19492014: coastDat2. Earth System Science Data 9(2):955–968, DOI 10.5194/essd-9-955-2017
Große F, Greenwood N, Kreus M, Lenhart HJ, Machoczek D, Pätsch J, Salt L, Thomas H (2016) Looking beyond stratification: a model-based analysis of the biological drivers of oxygen deficiency in the North Sea. Biogeosciences 13(8):2511–2535, DOI 10.5194/bg-13-2511-2016
Gutiérrez JLJ, Jones CGC, Strayer DLD, Iribarne OO (2003) Mollusks as ecosystem engineers: the role of shell production in aquatic habitats. Oikos 101:79–90, DOI 10.1034/j.1600-0706.2003.12322.x
Hill C, DeLuca C, Balaji V, Suarez M, Da Silva A (2004) The architecture of the Earth system modeling framework. Computing in Science and Engineering 6(1):18–28, DOI 10.1109/MCISE.2004.1255817
Ho A, Mbistrova A, Corb G (2016) The European offshore wind industry key 2015 trends and statistics. Tech. Rep. February, European Wind Energy Association, DOI 10.1109/CCA.1997.627749
Hofmeister R, Lemmen C, Kerimoglu O, Wirtz KW, Nasermoaddeli MH (2014) The predominant processes controlling vertical nutrient and suspended matter fluxes across domains - using the new MOSSCO system form coastal sea sediments up to the atmosphere. In: Lehfeldt R, Kopmann (eds) 11th International Conference on Hydroscience and Engineering, Hamburg, Germany, vol 28
Hofmeister R, Flöser G, Schartau M (2017) Estuary-type circulation as a factor sustaining horizontal nutrient gradients in freshwater-influenced coastal systems. Geo-Marine Letters 37(2):179–192, DOI 10.1007/s00367-016-0469-z
Howarth M (2001) North Sea circulation. In: Steele JH, Thorpe SA, Turekian KK (eds) Ocean Currents: A Derivative of the Encyclopedia of Ocean Sciences, Elsevier Science, London
Imhoff MLM, Bounoua L, Ricketts T, Loucks C, Harriss R, Lawrence WT (2004) Global patterns in human consumption of net primary production. Nature 429(June):870–873, DOI 10.1038/nature02685.Published
Inger R, Attrill MJ, Bearhop S, Broderick AC, James Grecian W, Hodgson DJ, Mills C, Sheehan E, Votier SC, Witt MJ, Godley BJ (2009) Marine renewable energy: Potential benefits to biodiversity? An urgent call for research. Journal of Applied Ecology 46(6):1145–1153, DOI 10.1111/j.1365-2664.2009.01697.x
International Renewable Energy Agency (2012) Renewable energy technologies: Cost analysis series. Tech. rep., International Renewable Energy Agency, Bonn
Joschko TJ, Buck B, Gutow L (2008) Colonization of an artificial hard substrate by Mytilus edulis in the German Bight. Marine Biology
Kaiser MJ, Clarke K, Hinz H, Austen M (2006) Global analysis of response and recovery of benthic biota to fishing. Marine Ecology Progress Series 311:1–14
Kaldellis J, Kapsali M (2013) Shifting towards offshore wind energy - Recent activity and future development. Energy Policy 53:136–148
Kerckhof F, Rumes B, Norro A, Houziaux J (2012) A comparison of the first stages of biofouling in two offshore wind farms in the Belgian part of the North Sea. In: Degraer S, Brabant R, Rumes B (eds) Offshore wind farms in the Belgian Part of the North Sea: Heading for an understanding of environmental impacts, Royal Belgian Institute of Natural Sciences, Brussels, chap 3, pp 17–39

Kerimoglu O, Hofmeister R, Maerz J, Riethmüller R, Wirtz KW (2017) The acclimative biogeochemical model of the southern North Sea. Biogeosciences 14(19):4499–4531, DOI 10.5194/bg-14-4499-2017

Klingbeil K, Burchard H (2013) Implementation of a direct nonhydrostatic pressure gradient discretisation into a layered ocean model. Ocean Modelling 65:64–77, DOI 10.1016/j.ocemod.2013.02.002

Krause D, Thörnig P (2016) JURECA: General-purpose supercomputer at Jülich Supercomputing Centre. Journal of large-scale research facilities JLSRF 2(A62):A62, DOI 10.17815/jlsrf-2-121

Krone R (2012) Offshore Wind Power Reef Effects and Reef Fauna Roles. Phd thesis, University of Bremen

Krone R, Gutow L, Joschko TJ, Schröder A (2013) Epifauna dynamics at an offshore foundation - Implications of future wind power farming in the North Sea. Marine Environmental Research 85:1–12, DOI 10.1016/j.marenvres.2012.12.004

Langhamer O, Wilhelmsson D, Engström J (2009) Artificial reef effect and fouling impacts on offshore wave power foundations and buoysa pilot study. Estuarine, Coastal and Shelf Science 82(3):426–432, DOI 10.1016/j.ecss.2009.02.009

van Leeuwen SM, van der Molen J, Ruardij P, Fernand L, Jickells T (2013) Modelling the contribution of deep chlorophyll maxima to annual primary production in the North Sea. Biogeochemistry 113(1-3):137–152, DOI 10.1007/s10533-012-9704-5

Lemmen C, Hofmeister R, Klingbeil K, Nasermoaddeli MH, Kerimoglu O, Burchard H, Kösters F, Wirtz KW (2018) Modular System for Shelves and Coasts (MOSSCO v1.0) a flexible and multi-component framework for coupled coastal ocean ecosystem modelling. Geoscientific Model Development 11(3):915–935, DOI 10.5194/gmd-11-915-2018

Leonhard S, Pedersen J, Moeslund B, Spanggaard G (2006) Benthic Communities at Horns Rev Before, During and After Construction of Horns Rev Offshore Wind Farm: Final Report. Tech. rep., Vattenfall AS, Aarhus

Liaw A, Wiener M (2002) Classification and Regression by randomForest. R News 2,3:18–22

Lindeboom H, Kouwenhoven H, Bergman M, Bouma S, Brasseur S, Daan R, Fijn R, De Haan D, Dirksen S, Van Hal R (2011) Short-term ecological effects of an offshore wind farm in the Dutch coastal zone; a compilation. Environmental Research Letters 6(3):1–13

Lützen J (1999) Styela clava Herdman (Urochordata, Ascidiacea), a successful immigrant to North West Europe: ecology, propagation and chronology of spread. Helgoländer Meeresuntersuchungen 52:383–391, DOI 10.1007/BF02908912

Maar M, Nielsen TG, Bolding K, Burchard H, Visser AW (2007) Grazing effects of blue mussel Mytilus edulis on the pelagic food web under different turbulence conditions. Marine Ecology Progress Series 339:199–213, DOI 10.3354/meps339199

Maar M, Bolding K, Petersen JK, Hansen JL, Timmermann K (2009) Local effects of blue mussels around turbine foundations in an ecosystem model of Nysted offshore wind farm, Denmark. Journal of Sea Research 62(2-3):159–174, DOI 10.1016/j.seares.2009.01.008

McCombs M, Mulligan R, Boegman L (2014) Offshore wind farm impacts on surface waves and circulation in eastern Lake Ontario. Coastal Engineering 93:32–39, DOI 10.1016/j.coastaleng.2014.08.001

Nasermoaddeli M, Lemmen C, Stigge G, Kerimoglu O, Burchard H, Klingbeil K, Hofmeister R, Kreus M, Wirtz K, Kösters F (2017) A model study on the large-scale effect of macrofauna on the suspended sediment concentration in a shallow shelf sea. Estuarine, Coastal and Shelf Science in press, DOI 10.1016/j.ecss.2017.11.002

Nehls G, Witte S, Buttger H, Dankers N, Jansen J, Millat G, Herlyn M, Merkert A, Kristensen PS, Ruth M, Buschbaum C, Wehrmann A (2009) Beds of blue mussels and Pacific oysters. Thematic Report, Wadden Sea Ecosystem, vol 11. Common Wadden Sea Secretariat, Wilhelmshaven, Germany

Newell R (2004) Ecosystem influences of natural and cultivated populations of suspension-feeding bivalve molluscs: a review. Journal of Shellfish Research 23(1):51–62

Nielsen T, Maar M (2007) Effects of a blue mussel Mytilus edulis bed on vertical distribution and composition of the pelagic food web. Marine Ecology Progress Series 339:185–198

Norling P, Kautsky N (2007) Structural and functional effects of Mytilus edulis on diversity of associated species and ecosystem functioning. Marine Ecology Progress Series 351:163–175, DOI 10.3354/meps07033

Orbis Energy Centre (2013) Monopiles Support Structures, 4C Offshore 2013-5-5. Online ressource http://www.4coffshore.com/windfarms/monopiles-support-structures-aid4.html [accessed 2018-05-05], Lowestoft, United Kingdom

OSPAR Commission (2010) Intertidal Mytilus edulis beds on mixed and sandy sediments. In: Quality Status Report 2010: Case Reports for the OSPAR list of threatened and/or declining species and habitats Update, Convention for the Protection of the Marine Environment of the North-East Atlantic Commission, Texel

Otto L, Zimmerman J, Furnes G, Mork M (1990) Review of the physical oceanography of the North Sea. Netherlands Journal of Sea Research 26(2-4):161–238, DOI 10.1016/0077-7579(90)90091-T

Pätsch J, Kühn W (2008) Nitrogen and carbon cycling in the North Sea and exchange with the North AtlanticA model study. Part I. Nitrogen budget and fluxes. Continental Shelf Research 28(6):767–787, DOI 10.1016/j.csr.2007.12.013

Phillips SJ, Dudík M, Elith J, Graham CH, Lehmann A, Leathwick J, Ferrier S (2009) Sample selection bias and presence - only distribution models: implications for background and pseudo - absence data. Ecological Applications 19(1):181–197, DOI 10.1890/07-2153.1

Platis A, Siedersleben SK, Bange J, Lampert A, Bärfuss K, Hankers R, Cañadillas B, Foreman R, Schulz-Stellenfleth J, Djath B, Neumann T, Emeis S (2018) First in situ evidence of wakes in the far field behind offshore wind farms. Scientific Reports 8(1):2163, DOI 10.1038/s41598-018-20389-y

Prins T, Smaal A, Dame R (1997) A review of the feedbacks between bivalve grazing and ecosystem processes. Aquatic Ecology 31(4):349–359, DOI 10.1023/A:1009924624259

Purkiani K, Becherer J, Klingbeil K, Burchard H (2016) Wind-induced variability of estuarine circulation in a tidally energetic inlet with curvature. Journal of Geophysical Research: Oceans 121(5):3261–3277, DOI 10.1002/2015JC010945

Reise K, Schubert A (1987) Macrobenthic turnover in the subtidal Wadden Sea: The Norderaue revisited after 60 years. Helgoländer Meeresuntersuchungen 41(1):69–82, DOI 10.1007/BF02365100

Reubens J, Degraer S, Vincx M (2011) Aggregation and feeding behaviour of pouting (Trisopterus luscus) at wind turbines in the Belgian part of the North Sea. Fisheries Research 108(1):223–227, DOI 10.1016/j.fishres.2010.11.025

Ricciardi A, Bourget E (1998) Weight-to-weight conversion factors for marine benthic macroinvertebrates. Marine Ecology Progress Series 163:245–251

Riis A, Dolmer P (2003) The distribution of the sea anemone Metridium senile (L.) related to dredging for blue mussels (Mytilus edulis L.) and flow habitat. Ophelia 57(1):43–52, DOI 10.1080/00785236.2003.10409504

Riisgård HU, Kittner C, Seerup DF (2003) Regulation of opening state and filtration rate in filter-feeding bivalves (Cardium edule, Mytilus edulis, Mya arenaria) in response to low algal concentration. Journal of Experimental Marine Biology and Ecology 284(1-2):105–127, DOI 10.1016/S0022-0981(02)00496-3

Rijkswaterstaat (2017) Waterbase http://live.waterbase.nl, last accessed 2017-03-30

Seed R, Suchanek TH (1992) Population and community ecology of Mytilus. In: Gosling E (ed) The mussel Mytilus: Ecology, physiology, genetics, and culture, Elsevier, Amsterdam, chap 4, p 589

Soetaert K, Herman PM, Middelburg JJ (1996) A model of early diagenetic processes from the shelf to abyssal depths. Geochimica et Cosmochimica Acta 60(6):1019–1040, DOI 10.1016/0016-7037(96)00013-0

Suchanek TH (1978) The ecology of Mytilus edulis L. in exposed rocky intertidal communities. Journal of Experimental Marine Biology and Ecology 31(1):105–120, DOI 10.1016/0022-0981(78)90139-9

Thieltges D, Strasser M, Reise K (2003) The American slipper limpet Crepidula fornicata (L.) in the northern Wadden Sea 70 years after its introduction. Helgoländer Meeresuntersuchungen 57:27–33

Tillin HM, Hiddink JG, Jennings S, Kaiser MJ (2006) Chronic bottom trawling alters the functional composition of benthic invertebrate communities on a sea-basin scale. Marine Ecology Progress Series 318:31–45, DOI 10.3354/meps318031

Tougaard J, Tougaard S, Jensen RC, Jensen T, Teilmann J, Adelung D, Liebsch N, Museum M, Müller G (2006) No Title

Umlauf L, Burchard H (2005) Second-order turbulence closure models for geophysical boundary layers. A review of recent work. DOI 10.1016/j.csr.2004.08.004

Waite RP (1989) The nutritional biology of Perna canaliculus with special reference to intensive mariculture systems. Phd thesis, University of Canterbury, Christchurch, New Zealand

Walday M, Kroglund T (2002) The North Sea. Europe's biodiversity - biogeographical regions and seas. Tech. rep., European Environment Agency, Brussels

Weston K (2005) Primary production in the deep chlorophyll maximum of the central North Sea. Journal of Plankton Research 27(9):909–922, DOI 10.1093/plankt/fbi064

White P, Pickett S (1985) The Ecology of Natural Disturbance and Patch Dynamics. In: White P, Pickett S (eds) Academic Press, Academic Press, London, pp 3–13

Widdows J, Fieth P, Worrall CM (1979) Relationships between seston, available food and feeding activity in the common mussel Mytilus edulis. Marine Biology 50(3):195–207, DOI 10.1007/BF00394201

Wilhelmsson D, Malm T (2008) Fouling assemblages on offshore wind power plants and adjacent substrata. Estuarine, Coastal and Shelf Science 79(3):459–466

Wilson J, Elliott M (2009) The habitatcreation potential of offshore wind farms. Wind Energy 12(2):203–212

Wirtz KW, Eckhardt B (1996) Effective variables in ecosystem models with an application to phytoplankton succession. Ecological Modelling 92(1):33–53

Wirtz KW, Kerimoglu O (2016) Autotrophic Stoichiometry Emerging from Optimality and Variable Co-limitation. Frontiers in Ecology and Evolution 4, DOI 10.3389/fevo.2016.00131

Zhang W, Wirtz K (2017) Mutual Dependence Between Sedimentary Organic Carbon and Infaunal Macrobenthos Resolved by Mechanistic Modeling. Journal of Geophysical Research: Biogeosciences 122(10):2509–2526, DOI 10.1002/2017JG003909